4U 1909+07: a hidden pearl

Ingo Kreykenbohm[1,2], Felix Fürst[1,2], Laura Barrágan[1,2], Jörn Wilms[1,2], Richard E. Rothschild[3], Slawomir Suchy[3], Katja Pottschmidt[4,5]

[1] *Dr. Karl Remeis-Sternwarte Bamberg, Sternwartstrasse 7, 96049 Bamberg, Germany*
[2] *Erlangen Centre for Astroparticle Physics (ECAP), Erwin-Rommel-Str. 1, 91058 Erlangen, Germany*
[3] *Center for Astrophysics and Space Sciences, University of California, San Diego, La Jolla, CA 92093-0424, USA*
[4] *CRESST, University of Maryland, Baltimore County, 1000 Hilltop Circle, Baltimore, MD 21250, USA*
[5] *NASA Goddard Space Flight Center, Astrophysics Science Division, Code 661, Greenbelt, MD 20771, USA*

Abstract

We present a detailed spectral and timing analysis of the High Mass X-ray Binary (HMXB) 4U 1909+07 with *INTEGRAL* and *RXTE*. 4U 1909+07 is a persistent accreting X-ray pulsar with a period of approximately 605 s. The period changes erratically consistent with a random walk expected for a wind accreting system. *INTEGRAL* detects the source with an average of 2.4 cps (corresponding to 15 mCrab), but sometimes exhibits flaring activity up to 50 cps (i.e. 300 mCrab). The strongly energy dependent pulse profile shows a double peaked structure at low energies and only a single narrow peak at energies above 20 keV. The phase averaged spectrum is well described by a powerlaw modified at higher energies by an exponential cutoff and photoelectric absorption at low energies. In addition at 6.4 keV a strong iron fluorescence line and at lower energies a black body component are present. We performed phase resolved spectroscopy to study the pulse phase dependence of the spectral parameters: while most spectral parameters are constant within uncertainties, the blackbody normalization and the cutoff folding energy vary strongly with phase.

Keywords: X-rays: stars – stars: flare – stars: pulsars: individual: 4U 1909+07 – stars: magnetic fields

1 Introduction

4U 1909+07 (also known as X1908+07) was discovered with the *Uhuru* satellite as 3U 1912+07 (in the third Uhuru catalog, Giacconi et al. 1974). Since then, the source was detected with most X-ray instruments. The nature of the system was, however, not clear for 30 years. Only in 2000, Wen et al. (2000) found a stable 4.4 d period in *RXTE* ASM data, which was interpreted as the orbital period of a binary system. The photoelectric absorption was found to vary by a factor of at least 3 with orbital phase (Levine et al. 2004). Such a behavior can be well described by a spherical wind model and an inclination of $54° \leq i \leq 70°$, depending on the parameters of the wind model. Furthermore, 4U 1909+07 shows irrgular flaring activity due to inhomogeneities in the wind of the donor star, which lead to different accretion rates.

In 2005, Morel & Grosdidier (2005) detected an OB star in the near infrared at the location of the X-ray source, thus confirming that the system is indeed a High Mass X-ray Binary (HMXB). They estimated the distance to the source to 7 kpc (Morel & Grosdidier 2005).

Using a pointed *RXTE*-PCA observation, Levine et al. (2004) discovered a period of ~605 s, explained as the pulse period of a rotating neutron star with an offset magnetic axis. Levine et al. (2004) were thus able to refine the binary orbit parameters. They obtained $M_\star = 9$–$31\,M_\odot$ and $R_\star \leq 22\,R_\odot$ for the mass and radius of the companion star assuming the canonical mass of $1.4\,M_\odot$ for the neutron star.

In this paper, we present the data and data reduction methods in Sect. 2. In Sect. 3 we analyze the pulse period evolution and the pulse profiles and in Sect. 4 we address the spectral properties of the source. We summarize and discuss our results in Sect. 5.

2 Data and Observations

We used all publicly available data of 4U 1909+07 from the International Gamma Ray Laboratory (*INTEGRAL*, Winkler et al. 2003) and the Rossi X-ray Timing Explorer (*RXTE*, Jahoda et al. 1996).

INTEGRAL has three X-ray science instruments, which provide coverage from 3 keV up to 10 MeV: the imager IBIS/ISGRI (Ubertini et al. 2003, 20 keV to 800 keV) with moderate energy resolution and a large effective area, the spectrometer SPI (20 keV to 10 MeV; Vedrenne et al. 2003) with excellent spectral

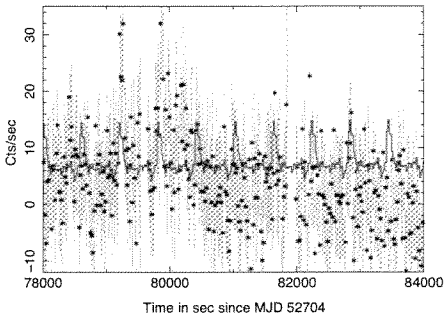

Figure 1: Closeup on an ISGRI lightcurve of 4U 1909+07 in the 20–40 keV with 20 s time resolution. The red line shows the folded pulse profile.

resolution suitable for the analysis of nuclear lines, and the X-ray monitor JEM-X (Lund et al. 2003, 3 keV to 35 keV). Thanks to ISGRI's large field of view of almost $30^\circ \times 30^\circ$ more than 6 Msec of data on 4U 1909+07 exist, mostly from the *INTEGRAL* core programme (Winkler 2001) and the GRS 1915+105 monitoring (Rodriguez & Bodaghee 2008), however, 4U 1909+07 was almost never in the field of view of JEM-X, as no observations were pointed directly at 4U 1909+07.

Among the detected sources in the field of view are prominent sources like GRS 1915+105 or SS 433. In total, twelve sources with a significance $> 6\sigma$ were detected in the field of view, with 4U 1909+07 being the fourth brightest source. In addition to the standard pipelines of the Offline Scientific Analysis software (OSA) version 7.0 for images and spectra, the `ii_light` distributed with OSA was used to obtain light curves with a higher temporal resolution. We used a time resolution of 20 s to maintain an acceptable signal-to-noise ratio and to obtain a good enough time resolution to measure the pulse period.

In addition to the *INTEGRAL* observations, we also used the observations of 4U 1909+07 performed by RXTE. Both major instruments of *RXTE*, the Proportional Counter Array (PCA; Jahoda et al. 2006), sensitive in the 2–60keV energy band and the High Energy X-Ray Timing Experiment (HEXTE; Rothschild et al. 1998), sensitive between 15–250 keV, were fully operational at that time. Both instruments have a large effective area and a high temporal resolution, but no imaging capabilities. In total, 196 ksec of *RXTE* data on 4U 1909+07 are available.

3 Timing Analysis

3.1 Pulse period evolution

Apart from the discovery of the pulsations based on *RXTE* data in 2000 and 2004 (Levine et al. 2004), no other measurements of the pulse period of 4U 1909+07 are available. The extensive archival *INTEGRAL* data are therefore optimal to track the evolution of the pulse period since 2003. We split the lightcurve into segments between 300 ksec and 800 ksec length to determine the period accurately. We then used epoch folding (Leahy et al. 1983) to determine the pulse period for each of these segments individually. 4U 1909+07 shows very strong pulse-to-pulse variations such that the actual pulse can not be seen by the naked eye (see, e.g., Fig. 1). Only after folding 500–1000 pulses, a stable pulse profile emerges which allows for a reliable pulse period determination. The pulse profile itself, however, is remarkably stable on longer time scales. A similar effect is seen in Vela X-1, although the overall luminosity is much higher in that source (Staubert et al. 1980).

The evolution of the pulse period since 2001 is shown in Fig. 2. The overall behvior is best described by a random walk model, but also a spin-up trend between March 2003 and April 2006 and a spin-down trend from April 2006 to October 2007 could describe the data. To confirm the random walk behavior, we implemented the algorithm proposed by de Kool & Anzer (1993): this algorithm evaluates the relative change in the pulse period P over different time intervals δt between individual measurements. In the case of a perfect random walk, the result will be a straight line with a slope of 0.5 in the $\log \delta\omega - \log \delta t$ space, where ω is the angular velocity: $\omega = 2\pi/P$. Fig. 3 shows the corresponding diagram for 4U 1909+07. Superimposed is a line with slope of 0.5, shifted in y-direction to fit the data. It is obvious that the line matches the data very well. The uncertainties in Fig. 3 include uncertainties of the determined pulsed

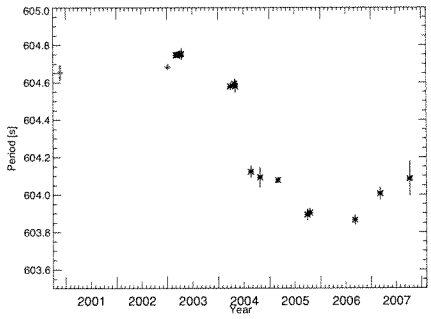

Figure 2: Evolution of the pulse period of 4U 1909+07. The historic *RXTE* data points of Levine et al. (2004) are shown as red crosses, our measurements obtained with *INTEGRAL* are shown as stars.

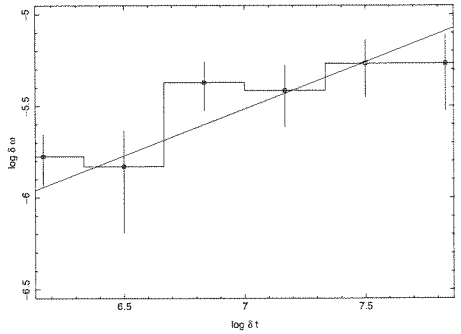

Figure 3: Pulse period evolution in $\log \delta\omega - \log \delta t$ space, as proposed by de Kool & Anzer (1993).

periods and also the uneven and coarse sampling.

3.2 Pulsprofiles

As shown by Levine et al. (2004), the 3.7 – 17 keV pulse profile shows two distinct peaks, with the second peak being slightly broader than the first peak and having a complex shape with two subpeaks at phase $\phi = 0.85$ and $\phi = 0.1$. To study the energy dependence of the pulse profile, we extracted pulse profiles from PCA data in different energy bands, using a period of $P = 604.685$ s and 32 phase bins. Thanks to the large effective area of the PCA instrument, high quality pulse profiles could be extracted in 30 narrow energy bands. Three energy bands are shown as an example in the upper three panels of Fig. 4. The pulse profiles show a smooth transition from a two peaked profile at low energies to a single peak profile at high energies. At energies below 5 keV the secondary peak is broader and stronger than the primary peak (Fig. 4a). With increasing energy both peaks become at first equally strong and more clearly separated and then the relative strength of the secondary peak declines further (Fig. 4b,c) . To obtain the pulse profile at high energies between 20 keV and 40 keV, we used *INTEGRAL* data taken in 2004. We used the same epoch as for the PCA analysis, but a period of $P = 604.747$ s, as determined by our analysis of the *INTEGRAL*-data. In this energy band, the secondary peak does not exist anymore while the primary pulse is clearly seen and has a sharp peak (Fig. 4d). The deep minimum around phase 0.3, however, is not energy dependent.

4 Spectral analysis

4.1 Phase averaged spectrum

The pulse phase averaged spectrum of 4U 1909+07 is best described by a powerlaw continuum attenuated by photoelectric absorption at low energies and an exponential turnover at high energies similar to most

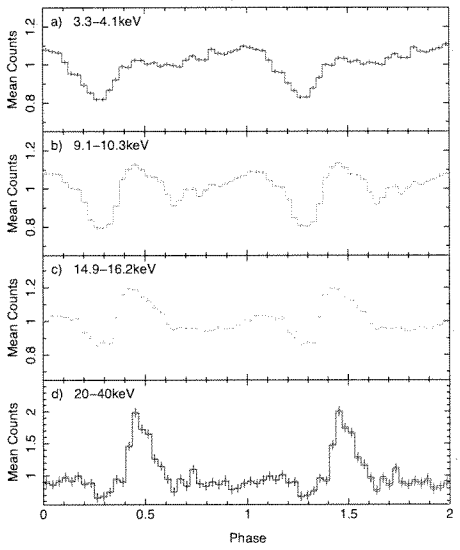

Figure 4: Energy resolved pulse profi les with *RXTE* PCA (**a** – **c**) and *INTEGRAL* ISGRI (**d**). The profi les are shown twice for clarity. Note that the *RXTE* and *INTEGRAL* profi les are not strictly phase aligned.

accreting X-ray pulsars. Levine et al. (2004) modeled the spectrum using bremsstrahlung which describes the data equally well. The turnover at high energies is often modeled with the `cutoffpl`, `highecut`, or the `fdcut` (Tanaka 1986). The `npex` model (Mihara 1995) is more complex as it involves a second powerlaw. Furthermore at 6.4 keV an iron fluorescence line is present.

We discarded all observations between orbital phase $0.88 < \phi_{\rm orb} < 0.12$, as the $N_{\rm H}$ is dramatically increased during this part of the orbit (Levine et al. 2004). We applied the typical continum models (see above) to the *RXTE* and *INTEGRAL* data (see Table 1). All models can describe the data almost equally well. In the case of the `fdcut` model, however, the cutoff energy is set to <1 keV, thus effectively removing the cutoff. We therefore did not use the `fdcut` model any more for 4U 1909+07. Independent of the applied continuum models, however, a soft excess below 10 keV is evident, which can be very well modeled using a blackbody with a temperature of $kT \approx 1.4$ keV. Fig. 5 shows the spectrum and the best fi t `cutoffpl` model.

4.2 Phase resolved spectra

Since the *INTEGRAL* ISGRI data did not provide high enough statistics for high resolution phase resolved spectroscopy, we only used the *RXTE* data. We divided the PCA and HEXTE data into 7 phasebins (see Fig. 6a). We applied a `cutoffpl` with an additional black body component to all phase bins. Neither the photoelectric absorption nor the power law index Γ varies with pulse phase. The cutoff folding energy, however, is highest in the primary peak with ~ 19 keV, while it is only ~14 keV during the secondary peak, explaining why the primary peak is much stronger at higher energies.

The black body component is strongly variable: the normalization changes by a factor of ~3. The blackbody is strongest between the two peaks and weakest in the rise and maximum of the primary peak. The temperature kT of the black body on the other hand does not change with pulse phase.

5 Discussion & Conclusion

We have presented a detailed study with *INTEGRAL* and *RXTE* of 4U 1909+07. We have shown that the pulse period changes strongly with time. The evolution of the period is best described by a random walk. Such a behavior has been seen in many other HMXBs like Vela X-1 and is a strong indicator for a direct accretion from the stellar wind of the optical companion without a persistent accretion disk (Ghosh & Lamb 1979). An accretion disk would provide a more constant transfer of angular momentum and thus a long-term spin-up or spin-down trend, as seen in other sources like 4U 1907+09 (Fritz et al. 2006).

Table 1: Fit parameters for various model of the phase averaged spectrum of 4U 1909+07.

Model parameter	Cutoffpl	Cutoffpl +bbody	Highecut
χ^2_{red}	1.76	1.01	1.07
N_H [atoms cm^{-2}]	$15.3^{+0.6}_{-0.5}$	$4.7^{+1.6}_{-1.9}$	$4.8^{+0.9}_{-1.6}$
Γ^1	$1.63^{+0.13}_{-0.02}$	$0.96^{+0.03}_{-0.06}$	$1.37^{+0.03}_{-0.08}$
Fe σ	$1.7^{+0.1}_{-0.5}$	$0.28^{+0.15}_{-0.11}$	$0.41^{+0.07}_{-0.06}$
Fe Energy [keV]	$6.4^{+0.8}_{-0.2}$	$6.40^{+0.04}_{-0.06}$	$6.39^{+0.04}_{-0.03}$
Fe Norm	$(1.1^{+0.1}_{-0.6}) \times 10^{-3}$	$(0.57^{+0.17}_{-0.11}) \times 10^{-3}$	$(0.78^{+0.07}_{-0.04}) \times 10^{-3}$

Model parameter	Highecut +bbody	NPEX	NPEX +bbody
χ^2_{red}	0.91	1.44	0.93
N_H [atoms cm^{-2}]	$6.8^{+2.0}_{-0.8}$	$1.7^{+0.7}_{-1.7}$	5^{+1}_{-3}
Γ^2	1.32 ± 0.10	$0.36^{+0.05}_{-0.15}$ / $-3.08^{+0.13}_{-0.09}$	$0.80^{+0.06}_{-0.15}$ / -2.0[3]
Fe σ	0.2 ± 0.2	$0.41^{+0.07}_{-0.06}$	$0.27^{+0.12}_{-0.18}$
Fe Energy [keV]	$6.39^{+0.04}_{-0.05}$	$6.37^{+0.04}_{-0.03}$	6.40 ± 0.05
Fe Norm	$(5^{+3}_{-1}) \times 10^{-4}$	$(0.80^{+0.07}_{-0.06}) \times 10^{-3}$	$(0.6^{+0.3}_{-0.1}) \times 10^{-3}$

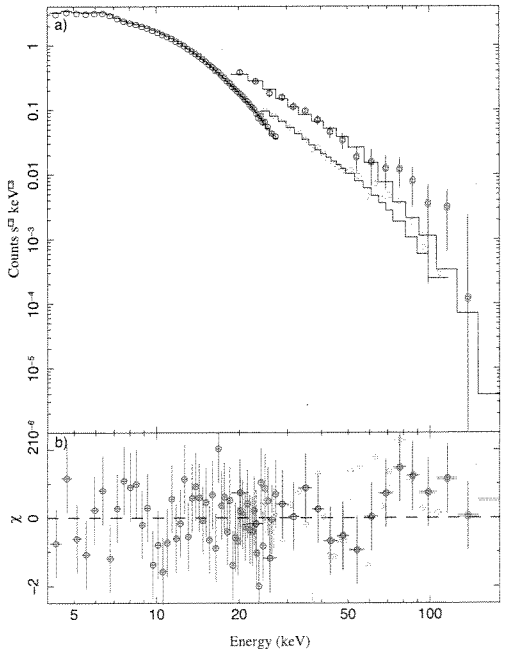

Figure 5: **a** Combined *RXTE* PCA (red) and HEXTE (blue) and *INTEGRAL* ISGRI (green) spectrum. The best fi t `cutoffpl`-model is also shown. **b** Residuals of the best fi t showing no evident deviation.

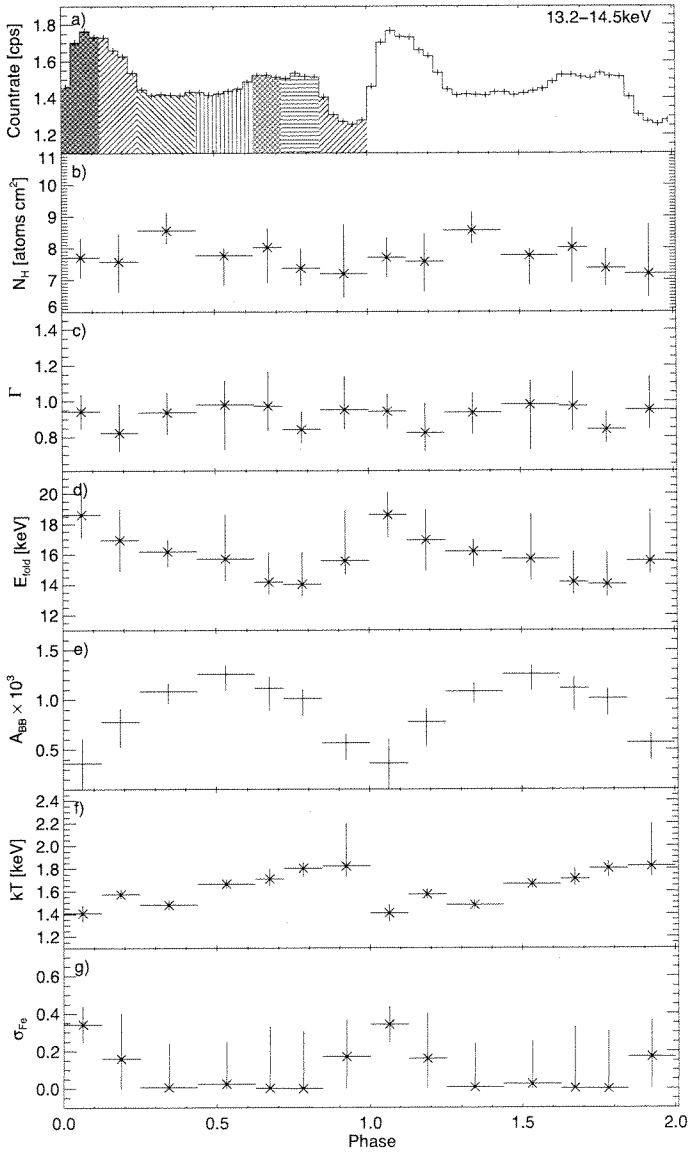

Figure 6: Spectral parameters of phase-resolved spectra **b** Pulse profi le in the 13.2-14.5 keV energy range. The different shaded areas indicate the phasebins. **b** Photoelectric absorption column $N_{\rm H}$, **c** Power law index Γ, **d** Folding energy, **e** Black body normalization, **f** Black body temperature, and **g** width of the Iron line.

Since the accreting neutron star is strongly magnetized (as indicated by strong coherent pulsations), the accreted matter has to couple to the magnetic fi eld thus inhibiting the formation of an accretion disk close to the neutron star. The required B fi eld strength is of the order of 10^{12} G. Such magnetic fi eld strengths are commonly observed in neutron stars, especially pulsars. In such a strong magnetic fi eld, however, cyclotron resonant scattering features (CRSFs) are expected to be present in the X-ray spectrum, as in the spectrum of Vela X-1 (Kreykenbohm et al. 2002) or MXB 0656−072 (McBride et al. 2006). Unfortunately, we found no evidence for a CRSF in 4U 1909+07 and are thus unable to determine the strength of the magnetic fi eld. However, the absence of CRSFs in the X-ray spectrum does not rule out the presence of a strong magnetic fi eld in 4U 1909+07, as CRSFs can be fi lled up again by photon spawning and depend strongly on the geometry of the accretion column and on the viewing angle (Schönherr et al. 2007).

The two distinct peaks in the pulse profi le at low energies suggest that the neutron star is accreting on both magnetic poles. However, the dramatic change of the pulse shape with energy suggests that the physical conditions in the accretion columns above the two poles might be different. The exact geometry of the accretion column, however, depends strongly on the way the matter couples to the magnetic fi eld and is highly uncertain (Basko & Sunyaev 1976; Meszaros 1984). Besides a simple fi lled funnel other possible confi gurations exist including a hollow or a partly hollow funnel and several small funnels.

These models, however, have to be taken with a pinch of salt, as the behavior of relativisitc plasma in magnetic fi elds with $B \approx 10^{12}$ G is still only little understood. Additionally gravitational light bending must be taken into account when analyzing pulse profi les and their origin (Kraus et al. 2003).

References

Basko, M. M. & Sunyaev, R. A. 1976, MNRAS, 175, 395

de Kool, M. & Anzer, U. 1993, MNRAS, 262, 726

Fritz, S., Kreykenbohm, I., Wilms, J., et al. 2006, A&A, 458, 885

Ghosh, P. & Lamb, F. K. 1979, ApJ, 234, 296

Giacconi, R., Murray, S., Gursky, H., et al. 1974, ApJS, 27, 37

Jahoda, K., Markwardt, C. B., Radeva, Y., et al. 2006, ApJS, 163, 401

Jahoda, K., Swank, J. H., Giles, A. B., et al. 1996, in EUV, X-Ray and Gamma-Ray Instrumentation for Astronomy VII, ed. O. H. W. Siegmund & M. A. Gummin, SPIE 2808, 59–70

Kraus, U., Zahn, C., Weth, C., & Ruder, H. 2003, ApJ, 590, 424

Kreykenbohm, I., Coburn, W., Wilms, J., et al. 2002, A&A, 395, 129

Leahy, D. A., Darbo, W., Elsner, R. F., et al. 1983, ApJ, 266, 160

Levine, A. M., Rappaport, S., Remillard, R., & Savcheva, A. 2004, ApJ, 617, 1284

Lund, N., Budtz-Jørgensen, C., Westergaard, N. J., et al. 2003, A&A, 411, L231

McBride, V. A., Wilms, J., Coe, M. J., et al. 2006, A&A, 451, 267

Meszaros, P. 1984, Space Sci. Rev., 38, 325

Mihara, T. 1995, PhD thesis, RIKEN, Tokio

Morel, T. & Grosdidier, Y. 2005, MNRAS, 356, 665

Rodriguez, J. & Bodaghee, A. 2008, ArXiv e-prints, 801

Rothschild, R. E., Blanco, P. R., Gruber, D. E., et al. 1998, ApJ, 496, 538

Schönherr, G., Wilms, J., Kretschmar, P., et al. 2007, A&A, 472, 353

Staubert, R., Kendziorra, E., Pietsch, W., C. Reppin, J. T., & Voges, W. 1980, ApJ, 239, 1010

Tanaka, Y. 1986, in Radiation Hydrodynamics in Stars and Compact Objects, ed. D. Mihalas & K.-H. A. Winkler, IAU Coll. 89, Heidelberg, 198

Ubertini, P., Lebrun, F., Di Cocco, G., et al. 2003, A&A, 411, L131

Vedrenne, G., Roques, J.-P., Schönfelder, V., et al. 2003, A&A, 411, L63

Wen, L., Remillard, R. A., & Bradt, H. V. 2000, ApJ, 532, 1119

Winkler, C. 2001, in Exploring the Gamma-Ray Universe, ed. A. Gimenez, V. Reglero, & C. Winkler, ESA SP-459, Alicante, 471

Winkler, C., Courvoisier, T. J.-L., Di Cocco, G., et al. 2003, A&A, 411, L1